Comparative Study of Photoluminescence Characteristics of Ag-Dy^{3+} Co-doped Host Matrices (Silica Xerogels and PVA Films)

Tabarak A. Al-Mashhadani [1], Firas J. Kadhim [2]

[1] Institute of Laser for Postgraduate Studies, University of Baghdad, Baghdad, Iraq
[2] Department of Physics, College of Science, University of Baghdad, Baghdad, IRAQ

Abstract
In this study, silica xerogels and poly vinyl alcohol films doped with Ag-Dy^{3+} at specific concentration of silver nanoparticles (Ag NPs) where synthesized using sol-gel route and chemical method. Spectroscopic analysis of Ag NPs in both hosts revealed a distinct surface plasmon resonance (SPR) band centered at the special range from 426 to 429 nm. Absorption and photoluminescence (PL) spectra were recorded at room temperature, as a function of Dy^{3+} concentration. Prominent emission bands from Dy^{3+} ions were observed at $^4F_{9/2}\rightarrow{}^6H_{13/2}$ and $^4F_{9/2}\rightarrow{}^6H_{15/2}$ under 350 nm excitation. It was demonstrated that the presence of Ag NPs significantly enhanced the PL intensity of Dy^{3+} ions. This enhancement is attributed to the strong local electric field generated by the SPR effect such as nanoparticles, which facilitates efficient energy transfer to the Dy^{3+} ions. Consequently, the emission cross-section increases with concentration up to 0.0055% for silica xerogels, and the same behavior of PVA films was seen at up to 0.0086%.

Keywords: Photoluminescence; Spectroscopy; Surface plasmon resonance; Inorganic host; Organic host
Received: 05 January 2025; **Revised:** 11 February 2025; **Accepted:** 18 February 2025; **Published:** 1 April 2025

1. Introduction

One of the best rare earth activators is the trivalent ion Dy^{3+}, which exhibits strong luminescence in a range of lattices and both blue and yellow emissions. These colors are essential for the development of white light emission and are useful in optical display systems and light emitting diodes (LEDs). To determine the overall emission in the white light zone, one can adjust the yellow-to-blue emission intensity ratio (Y/B). Generally speaking, Dy^{3+} shows three distinct emission bands: the blue emission at 480 nm, which corresponds to the $^4F_{9/2}\rightarrow{}^6H_{15/2}$ transition; the yellow emission at 577 nm, which corresponds to the hypersensitive transition $^4F_{9/2}\rightarrow{}^6H_{13/2}$ ($\Delta J=2$); and the weak red emission at 670 nm, which corresponds to the transition $^4F_{9/2}\rightarrow{}^6H_{11/2}$ [1,2].

Rare earths (REs) have a low emission efficiency because of their extremely narrow absorption cross section. The scientific community is employing a number of tactics to get around this restriction. One of the best methods for increasing the emission efficiency of RE ions through an increase in the absorption cross sections is co-doping with metal nanoparticles (NPs) [3]. The electric field surrounding metal nanoparticles is greatly enhanced when they display SPR or localized surface plasmon resonance (LSPR). The electric field around RE ions near the metal NPs is strengthened as a result of the action. These lead to an increase in the cross section of RE absorption, which in turn helps to improve PL [4]. This phenomenon has been successfully applied to matrices doped with RE. The size, shape, spatial orientation, and coupling distance between the metal NPs and RE ions, as well as the embedded dielectric medium, all have a significant impact on the LSPR effect [5-9]. When the RE ions are within 10 nm of the metal NPs, they experience an electric field that is approximately 100 times stronger than the incident field. This changes the spectrum characteristics of the RE ions and raises their excitation rates [10].

Ag co-doped with lanthanide elements has been synthesized using a variety of techniques, such as the sol–gel process, which is nearly well-organized and has good dopant dispersion [11]. Compared to other inorganic complexes, polymer-rare earth complexes offer additional benefits such transparency, superior mechanical qualities, simplicity of production, light weight, and design flexibility [12].

This study focuses on PL characteristics of Dy^{3+} ions at different concentrations in Ag- Dy^{3+} co-doped at specific concentration of Ag NPs in two host structural materials: silica matrices and PVA films.

2. Experimental Part

A specific concentration of 5×10^{-3} mol/L and a reduction time of 5 minutes after the broiling point were

used to prepare Ag colloids [13]. Dy^{3+} ions were obtained from dysprosium chloride hexahydrate ($DyCl_3.6H_2O$, 99.9% from Aldrich). 1.0×10^{-1} mol\L was obtained by dissolving $DyCl_3.6H_2O$ in deionized water to prepared different concentrations of Dy^{3+} solutions. A dilution equation was then used to lower this concentration to 2.0×10^{-2}, 35×10^{-3}, and 55×10^{-3} mol\L [14].

Optimal conditions were used to prepare the Ag-Dy^{3+} co-doped silica xerogels [13]. A magnetic stirrer was used to homogenize the mixture of TEOS (purity >98%) and absolute EthOH (C_2H_5OH), represented as sol (I), for 10 minutes after adding a $DyCl_3$ solution with varying concentrations of Dy^{3+} ions and an Ag NPs solution. Sol (II), which stands for the mixture of deionized water and 100% EthOH, was gradually added to sol (I) for the hydrolysis. The finished solution was stirred with a magnetic stirrer for 30 minutes at room temperature and for two hours at 60 °C. This was followed by the addition of 0.5 mL of N,N-dimethylformamide. A closed glass tube was filled with the resulting solution, which was then stored at room temperature (Fig. 1a) [15].

Ag-Dy^{3+} co-doped PVA with a molecular weight of 10000 g/mol (BDH Chemicals, England) were prepared. 1.5 g of PVA powder was added into 10 mL of distilled water and let to swell for 24 hours at ambient temperature. 2 mL of both Ag colloids and $DyCl_3.6H_2O$ solution were added to the polymeric solution and stirred continuously during the entire process. The final solution was meticulously dispensed into flat glass plate dishes. The procedure was conducted multiple times using varying concentrations of Dy^{3+} solutions. Homogenous films were obtained following 36 hours drying period in an air oven at 40°C as illustrated in Fig. (1b). The films thicknesses were measured and found to be in the range of 25±5µm.

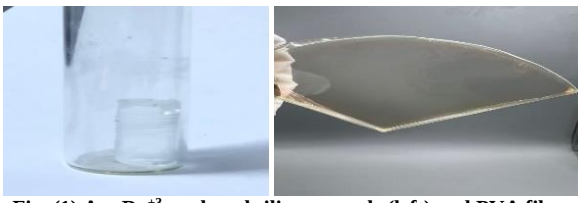

Fig. (1) Ag- Dy^{+3} co-doped silica xerogels (left) and PVA films (right) at specific concentration of Ag NPs 5×10^{-3} M

3. Results and Discussions

Figure (a) shows the absorption spectra of Ag-Dy^{3+} co-doped silica xerogels. A band at 213 nm is ascribed to the development of defects in the silica matrix, while other absorption bands range from 210 to 250 nm. Each spectra have eight Dy^{3+} ion absorption bands at 317, 352, 365, 374, 446, 750, 810, and 911 nm. The SPR of Ag NPs is detected at 429 nm. The 6P3/2 Dy^{3+} ion transition and the $^6H_{15/2}\rightarrow{}^4M_{17/2}$ transition are responsible for the absorption band at 317 nm. The bands located at 352, 365, and 446 nm correspond to the transitions of Dy^{3+} ions at $^6H_{15/2}\rightarrow{}^4I_{13/2}$, $^4F_{7/2}$, $^6H_{15/2}\rightarrow{}^4M_{15/2}$, $^6P_{7/2}$, and $^6H_{15/2}\rightarrow{}^4I_{11/2}$, respectively. The bands at 750, 810, and 911 nm are attributed to the transitions of Dy^{3+} active ions at $^6H_{15/2}\rightarrow{}^6F_{3/2}$, $^6H_{15/2}\rightarrow{}^6F_{5/2}$, and $^6H_{15/2}\rightarrow{}^6F_{7/2}$, respectively [16,17].

The peak of each band is increased as a result of a corresponding increase of concentration. Ag NPs result in an enhancement of the local electric field around the NPs. The energy transfer from Ag NPs to Dy^{3+} ions has also been recognized as a factor to enhance PL intensity ($Ag^+\rightarrow Dy^{3+}$) [18].

All Ag-Dy^{3+} co-doped PVA films with varying concentrations of Dy^{3+} ions and a specific Ag NPs concentration of 5×10^{-3} M have their absorption spectra in Fig. (2b). Each spectra comprises eight absorption bands, one of which corresponds to the SPR of Ag NPs at 426 nm and the other to intra-configuration 4f-4f transitions of the Dy^{3+} ions [14]. The existence of these bands in Ag-Dy^{3+} co-doped materials indicates the ions' spectroscopic activity [19].

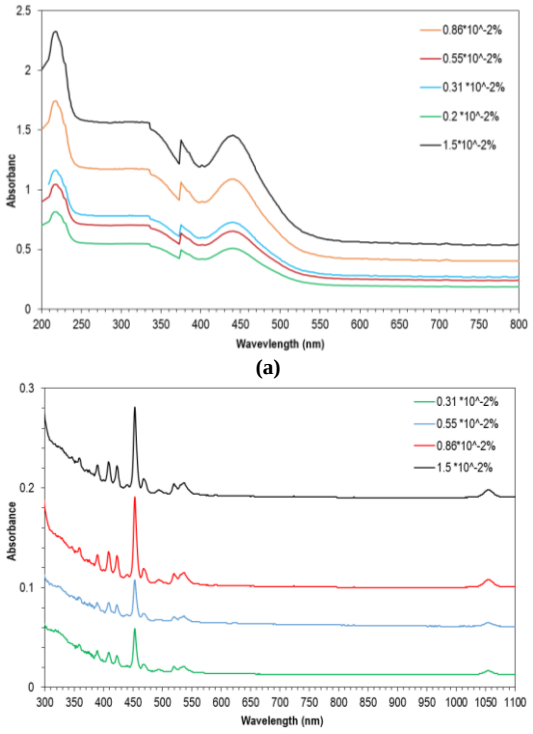

Fig. (2) Absorption spectra of Ag-Dy^{+3} co-doped (a) silica xerogels (b) PVA films at specific concentration of Ag NPs (5×10^{-3}M) and different concentrations of Dy^{3+}

Figure (3a) shows the PL spectra of Ag-Dy^{3+} co-doped silica xerogels when excited by 350 nm source. Emissions that peaked at 477, 576, and 518 nm, respectively, were found to be blue, yellow, and green simultaneously [20]. These are ascribed to the

$^4F_{9/2} \rightarrow {}^6H_{13/2}$ and $^4F_{9/2} \rightarrow {}^6H_{15/2}$ transitions [21]. When Dy^{3+} concentrations are high, the ions aggregate in the silica matrix's structural pores, reducing the intensity of photoluminescence. As a result, Ag NPs will enhance Dy^{3+} emission during energy transfer because of the surface plasmon resonance band [22].

The emission cross-section (σ_{em}) increases gradually with the increase in the Dy^{3+} ions concentration until reaching a maximum value of 0.0055%, then slightly decreases for the higher doping levels of Dy^{3+} ions (3.3-1.1) $\times 10^{-19}$ cm^2. The structural behavior of the Dy^{3+} ions and Ag in these matrices is described as randomly dispersed and unable to form any ligands in silica networks.

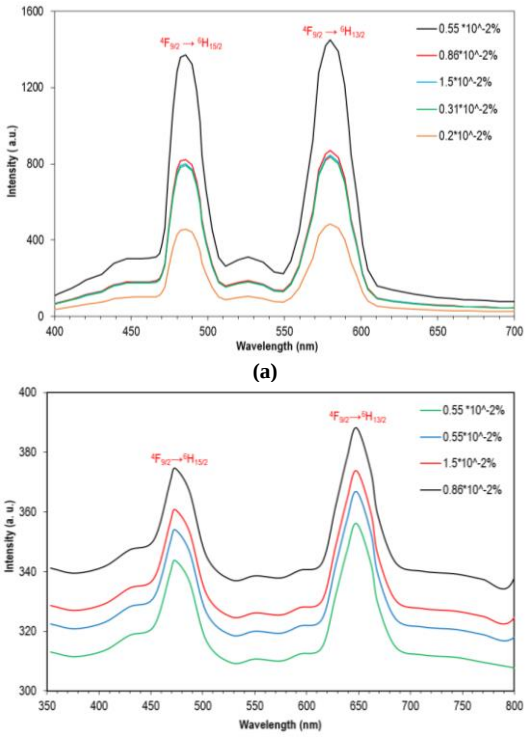

Fig. (3) PL spectra of Ag-Dy^{+3} co-doped (a) silica xerogels (b) PVA films at specific concentration of Ag NPs (5×10^{-3}M) and different concentrations of Dy^{3+}

Figure (b) shows PL spectra of the Ag NPs co-doped, Dy^{3+}:PVA films produced by excitation with 350 nm source. It is evident that the monoliths' PL intensity has grown. A possible explanation for this could be the local field effect (LFE) caused by the SPR of metallic nanoparticles. SPR polaritons are created by an oscillation of electrons moving across the surface of metal nanoparticles due to the difference in permittivity between the metal and the host [23,24]. Due to these oscillations, a restricted electromagnetic field is created near the NPs, increasing the local electric field surrounding them [25].

The emission cross-section (σ_{em}) slightly increases gradually with the increase in the Dy^{3+} ions concentration until reaching a maximum value for the concentration Dy^{3+} 0.0086% and then decreases slightly for higher doping levels of Dy^{3+} ions (2.8- 0.9) $\times 10^{-19}$ cm^2. The structural behavior of Dy^{3+} ions and silver nanoparticles within this host is characterized by random dispersion.

4. Conclusions

In conclusion, it was noted that the PVA films were characterized by optical transparency. It shoes no cracks whereas the silica xerogels suffered from shrinkages. The SPR effect of silver nanoparticles with Dy^{3+} ions were observed in co-doped with both media: inorganic host and organic host and its, play a key role in improving Dy^{3+} ions emission. Spectral analysis; based on emission cross-section values—ranging from (3.3–1.1) $\times 10^{-19}$ cm^2 for silica xerogels and (2.8–0.9) $\times 10^{-19}$ cm^2 for PVA films, demonstrated that the inorganic host exhibited superior photoluminescence characteristics.

References

[1] Y. Lian et al., J. Rare Earths, 39(8) (2021) 889-896.
[2] M.K. Hossain et al., ACS Appl. Electro. Mater., 3(9) (2021) 3715-3746.
[3] N. Dehingia et al., J. Lumines., 227 (2020) 117510.
[4] N. Shasmal and B. Karmakar, J. Non-Cryst. Solids, 463 (2017) 40-49.
[5] S.Q. Mawlud et al., Opt. Mater., 69 (2017) 318-327.
[6] R. Sharma and A.S. Rao, Opt. Mater., 84 (2018) 375-382.
[7] I.I. Kindrat et al., J. Lumines., 213 (2019) 290-296.
[8] N.M. Yusoff, M.R. Sahar, and S.K. Ghoshal, J. Mol. Struct., 1079 (2015) 167-172.
[9] J.A. Jiménez, Solid State Commun., 15(40) (2013) 17587-17594.
[10] A.C. Marques and R.M. Almeida, J. Non-Cryst. Solids, 353(27) (2007) 2613-2618.
[11] F.F. Al-Harbi and J.M. El Ghoul, Cond. Matter, 6 (2021) 24-35.
[12] R. Decadt et al., Inorg. Chem., 51 (2012) 11623–11634.
[13] T.A. Al-Mashhadani and F.J. Al-Maliki, Iraqi J. Appl. Phys., 18(3) (2022) 25-30.
[14] T.A. Al-Mashhadani and F.J. Kadhim, J. Sol-Gel Sci. Technol., 106(2) (2023) 553-560.
[15] T.A. Mashhadani, F.J. Kadhim, and N.A. Hashim, Iraqi J. Appl. Phys., 20(2B) (2024) 465-468.
[16] S. Singla et al., Opt. Mater., 126 (2022) 112236.
[17] A. Mastanappa et al., Opt. Mater., 157 (2024) 116224.
[18] S.H. Hasan and S.S.M. Alawadi, Iraqi J. Sci., 63(5) (2022) 2025-2038.
[19] A.S. Altowyan et al., Ceram. Int., 50(9) (2024) 14529-14541.
[20] J.A. Jiménez and M. Sendova, Solid State Commun., 152(18) (2012) 1786-1790.
[21] H.S. Albaqawi et al., J. Alloys Comp., 965 (2023) 171101.
[22] V.L. Paperny et al., J. Lumines., 279 (2025) 121044.
[23] S.K. Gupta et al., Opt. Mater., 35(11) (2013) 2320-2328.
[24] S.K. Gupta et al., Int. J. Appl. Ceram. Technol., 10(6) (2013) 593-602.
[25] W. Xu, X. Chen, and H. Song, Nano Today, 17 (2017) 54-78.

